arXiv:1601.03233v2 [hep-ph] 6 Apr 2016

Hidden-charm molecular pentaquarks and their charm-strange partners

Rui Chen[a,b], Xiang Liu[a,b], Shi-Lin Zhu[c,d,e]

[a] *School of Physical Science and Technology, Lanzhou University, Lanzhou 730000, China*
[b] *Research Center for Hadron and CSR Physics, Lanzhou University and Institute of Modern Physics of CAS, Lanzhou 730000, China*
[c] *School of Physics and State Key Laboratory of Nuclear Physics and Technology, Peking University, Beijing 100871, China*
[d] *Collaborative Innovation Center of Quantum Matter, Beijing 100871, China*
[e] *Center of High Energy Physics, Peking University, Beijing 100871, China*

Abstract

In the framework of one-pion-exchange (OPE) model, we study the hidden-charm and charm-strange molecular pentaquark systems composed of a heavy baryon (Σ_c, Σ_c^*) and a vector meson $(\bar{K}^*, \bar{D}^*)$, where the S-D mixing effect is considered in our calculation. Our result shows that the $\Sigma_c\bar{D}^*$ molecular state with $(I = 1/2, J^P = 3/2^-)$ and the $\Sigma_c^*\bar{D}^*$ molecular state with $(I = 1/2, J^P = 5/2^-)$ exist in the mass range of the observed $P_c(4380)$ and $P_c(4450)$, respectively. Moreover, we predict two other hidden-charm molecular pentaquarks with configurations $\Sigma_c\bar{D}^*$ $(I = 3/2, J^P = 1/2^-)$ and $\Sigma_c^*\bar{D}^*$ $(I = 3/2, J^P = 1/2^-)$ and two charm-strange molecular pentaquarks $P_{cs}(3340)$ and $P_{cs}(3400)$ corresponding to the $\Sigma_c\bar{K}^*$ configuration with $(I = 1/2, J^P = 3/2^-)$ and the $\Sigma_c^*\bar{K}^*$ configuration with $(I = 1/2, J^P = 5/2^-)$, respectively. Additionally, we also predict some hidden-bottom $\Sigma_b^{(*)}B^*$ and B_c-like $\Sigma_c^{(*)}B^*/\Sigma_b^{(*)}\bar{D}^*$ pentaquarks.

Keywords:
Molecular pentaquark state, Exotic state, One pion exchange, S-D mixing
PACS: 12.39.Pn, 14.20.Pt

1. Introduction

One of the most important research topics of hadron physics is the search for the exotic states like the glueballs, hybrid mesons, and multiquark states. In the past decade, the experimental observations of many charmonium-like states have inspired extensive study of exotic hadronic states (see the recent review in Ref. [1]). Especially, the recent observation of $P_c(4380)$ and $P_c(4450)$ states by the LHCb Collaboration [2] in the $\Lambda_b^0 \to K^- J/\psi p$ process has aroused the theorists' strong interest in the hidden-charm pentaquark states. The resonance parameters of the two P_c states are [2]

$$\begin{aligned} M_{P_c(4380)} &= 4380 \pm 8 \pm 29\,\text{MeV}, & \Gamma_{P_c(4380)} &= 205 \pm 18 \pm 86\,\text{MeV}, \\ M_{P_c(4450)} &= 4449.8 \pm 1.7 \pm 2.5\,\text{MeV}, & \Gamma_{P_c(4450)} &= 39 \pm 5 \pm 19\,\text{MeV}. \end{aligned}$$

The preferred spin-parity quantum numbers of of $P_c(4380)$ and $P_c(4450)$ are $3/2^{\mp}$ and $5/2^{\pm}$, respectively. Before the observation of the two P_c states, hidden-charm pentaquarks have been predicted in Refs. [3, 4, 5, 6, 7, 8, 9, 10].

Until now, theoretical interpretations of $P_c(4380)$ and $P_c(4450)$ include the molecular pentaquark states [11, 12, 13, 14, 15, 16, 17, 18, 19], the diquark-diquark-antiquark pentaquark [20, 21, 22, 23, 24, 25], the diquark-triquark pentaquark [26, 27], the re-scattering effect [28, 29, 30], the topological soliton model [31], etc. With the molecular pentaquark assignment, the mass of $P_c(4450)$ and $P_c(4380)$ can be understood quite naturally [11].

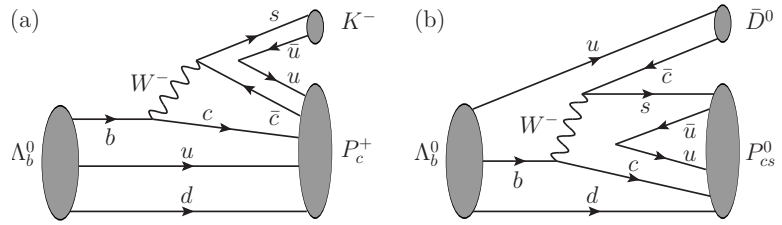

Figure 1: Feynman diagrams for $\Lambda_b^0 \to K^- P_c^+$ and $\Lambda_b^0 \to \bar{D}^0 P_{cs}^0$.

The tensor force mixes the S-D wave and plays a crucial role in the case of the deuteron. This S-D mixing effect was not included in Ref. [11]. In the present work, we consider the S-D mixing effect to reexamine the hidden-charm $\Sigma_c(2455)\bar{D}^*$ and $\Sigma_c^*(2520)\bar{D}^*$ systems, which is an extension of Ref. [11].

As shown in Fig. 1, two $P_c(4380)$ and $P_c(4450)$ states are produced via Fig. 1 (a). However, there exists another combination of quarks in the final

state in Fig. 1 (b), where the charm-strange pentaquarks (the P_{cs} states) may also be produced. Compared with Fig. 1 (a), Fig. 1 (b) is not suppressed, which stimulates our interest in the charm-strange molecular pentaquarks composed of either $\Sigma_c\bar{K}^*$ or $\Sigma_c^*\bar{K}^*$.

We also study the hidden-bottom $\Sigma_b B^*$ and $\Sigma_b^* B^*$ molecular systems and B_c-like $\Sigma_c B^*/\Sigma_b\bar{D}^*$ and $\Sigma_c^* B^*/\Sigma_b^*\bar{D}^*$ molecular systems, which are the partners of the hidden-charm molecular pentaquarks.

This paper is organized as follows. After the introduction, we present the deduction of the OPE potentials in Section 2 and numerical results in Section 3. The last section is a short summary.

2. The effective potential

In the following, we derive the OPE effective potentials of the hidden-charm $\Sigma_c\bar{D}^*$ and $\Sigma_c^*\bar{D}^*$ molecular systems, and charmed-strange $\Sigma_c\bar{K}^*$ and $\Sigma_c^*\bar{K}^*$ molecular systems.

2.1. Wave function

In this subsection, we construct the wave functions of the hidden-charm $\Sigma_c\bar{D}^*$ and $\Sigma_c^*\bar{D}^*$ molecular systems and charmed-strange $\Sigma_c\bar{K}^*$ and $\Sigma_c^*\bar{K}^*$ molecular systems. For a system composed of two colorless hadrons, its total wave function is expressed as

$$|\Psi\rangle = \left|\frac{\phi(r)}{r}\right\rangle \otimes \left|^{2S+1}L_J\right\rangle \otimes |I, I_3\rangle, \tag{1}$$

where $|\phi(r)/r\rangle$, $|^{2S+1}L_J\rangle$ and $|I, I_3\rangle$ denote the radial, spin-orbit and flavor wave functions, respectively. The radial wave function will be obtained via numerical calculation in Sec. 3. Since the S-D mixing is taken into account, the orbital quantum number $L = 0$ or $L = 2$. The spin $S = 1/2$ and $3/2$ for the $\Sigma_c\bar{M}^*$ configuration, and $S = 1/2$, $3/2$ and $5/2$ for the $\Sigma_c^*\bar{M}^*$ configuration. Then, the spin-orbit wave function $|^{2S+1}L_J\rangle$ can be written as

$$\begin{aligned}
J = \tfrac{1}{2}: &\quad |^2\mathbb{S}_{\frac{1}{2}}\rangle, \quad |^4\mathbb{D}_{\frac{1}{2}}\rangle, \\
J = \tfrac{3}{2}: &\quad |^4\mathbb{S}_{\frac{3}{2}}\rangle, \quad |^2\mathbb{D}_{\frac{3}{2}}\rangle, \quad |^4\mathbb{D}_{\frac{3}{2}}\rangle, \\
J = \tfrac{5}{2}: &\quad |^6\mathbb{S}_{\frac{5}{2}}\rangle, \quad |^2\mathbb{D}_{\frac{5}{2}}\rangle, \quad |^4\mathbb{D}_{\frac{5}{2}}\rangle, \quad |^6\mathbb{D}_{\frac{5}{2}}\rangle.
\end{aligned} \tag{2}$$

The general expressions of the spin-orbit wave function $|^{2S+1}L_J\rangle$ for the $\Sigma_c\bar{M}^*$ and $\Sigma_c^*\bar{M}^*$ systems are

$$\begin{aligned}
\Sigma_c\bar{M}^*: \quad \left|^{2S+1}L_J\right\rangle &= \sum_{m,m',m_S m_L} C^{S,m_S}_{\frac{1}{2}m,1m'} C^{J,M}_{Sm_S,Lm_L} \chi_{\frac{1}{2}m}\epsilon^{m'}|Y_{L,m_L}\rangle, \\
\Sigma_c^*\bar{M}^*: \quad \left|^{2S+1}L_J\right\rangle &= \sum_{m,m',m_S m_L} C^{S,m_S}_{\frac{3}{2}m,1m'} C^{J,M}_{Sm_S,Lm_L} \Phi_{\frac{3}{2}m}\epsilon^{m'}|Y_{L,m_L}\rangle.
\end{aligned}$$

Here, $\chi_{\frac{1}{2}m}$ is the spin wave function and Y_{L,m_L} is the spherical harmonics function. $C^{J,M}_{Sm_S,Lm_L}$, $C^{S,m_S}_{\frac{1}{2}m,1m'}$ and $C^{S,m_S}_{\frac{3}{2}m,1m'}$ are the Clebsch-Gordan coefficients. The polarization vector for the $\bar{M}^*$ vector meson is defined as $\epsilon^m_\pm = \mp\frac{1}{\sqrt{2}}\left(\epsilon^m_x \pm i\epsilon^m_y\right)$ and $\epsilon^m_0 = \epsilon^m_z$, which satisfy $\epsilon_{\pm1} = \frac{1}{\sqrt{2}}(0,\pm1,i,0)$ and $\epsilon_0 = (0,0,0,-1)$. The polarization tensor $\Phi_{\frac{3}{2}m}$ for Σ_c^* is constructed as $\Phi_{\frac{3}{2}m} = \sum_{m_1,m_2}\langle\frac{1}{2},m_1;1,m_2|\frac{3}{2},m\rangle\chi_{\frac{1}{2},m_1}\epsilon^{m_2}$.

For the $\Sigma_c\bar{M}^*$ and $\Sigma_c^*\bar{M}^*$ systems, the flavor wave function $|I,I_3\rangle$ can be grouped into two categories since their isospin can be classified into either 1/2 or 3/2, i.e.,

$$\begin{cases}
\left|\frac{1}{2},\frac{1}{2}\right\rangle = \sqrt{\frac{2}{3}}\left|\Sigma_c^{(*)++}M^{*-}\right\rangle - \frac{1}{\sqrt{3}}\left|\Sigma_c^{(*)+}\bar{M}^{*0}\right\rangle \\
\left|\frac{1}{2},-\frac{1}{2}\right\rangle = \frac{1}{\sqrt{3}}\left|\Sigma_c^{(*)+}M^{*-}\right\rangle - \sqrt{\frac{2}{3}}\left|\Sigma_c^{(*)0}\bar{M}^{*0}\right\rangle
\end{cases}, \tag{3}$$

$$\begin{cases}
\left|\frac{3}{2},\frac{3}{2}\right\rangle = \left|\Sigma_c^{(*)++}\bar{M}^{*0}\right\rangle \\
\left|\frac{3}{2},\frac{1}{2}\right\rangle = \frac{1}{\sqrt{3}}\left|\Sigma_c^{(*)++}M^{*-}\right\rangle + \sqrt{\frac{2}{3}}\left|\Sigma_c^{(*)+}\bar{M}^{*0}\right\rangle \\
\left|\frac{3}{2},-\frac{1}{2}\right\rangle = \sqrt{\frac{2}{3}}\left|\Sigma_c^{(*)+}M^{*-}\right\rangle + \frac{1}{\sqrt{3}}\left|\Sigma_c^{(*)0}\bar{M}^{*0}\right\rangle \\
\left|\frac{3}{2},-\frac{3}{2}\right\rangle = \left|\Sigma_c^{(*)0}M^{*-}\right\rangle
\end{cases}, \tag{4}$$

where $\bar{M}^*$ is defined as $\bar{M}^* = \left(K^{*-},-\bar{K}^{*0}\right)^T$ or $\bar{M}^* = \left(\bar{D}^{*0},D^{*-}\right)^T$.

2.2. Lagrangians

In the derivation of the effective OPE potentials, we need the effective Lagrangain

$$\mathcal{L}_{\mathbb{P}} = ig\mathrm{Tr}\left[\bar{H}_a{}^{(\bar{Q})}\gamma^\mu A^\mu_{ab}\gamma_5 H_b^{(\bar{Q})}\right], \tag{5}$$

$$\mathcal{L}_{\mathcal{S}} = -\frac{3}{2}g_1\varepsilon^{\mu\nu\lambda\kappa}v_\kappa\mathrm{Tr}\left[\bar{\mathcal{S}}_\mu A_\nu \mathcal{S}_\lambda\right], \tag{6}$$

which was constructed by considering the heavy quark limit and chiral symmetry [32, 33, 34, 35, 36, 37]. Here, $H_a^{(\bar{Q})}$ stands for a multiplet field composed of the pseudoscalar meson $P^{(\bar{Q})} = (\bar{D}^0, D^-)^T$ and vector meson $P^{*(\bar{Q})} = (\bar{D}^{*0}, D^{*-})^T$ in Eq. (7). Its conjugate field satisfies $\bar{H}_a^{(\bar{Q})} = \gamma_0 H_a^{(\bar{Q})\dagger}\gamma_0$. $\mathcal{S}_\mu$ is the superfield composed of Dirac spinor fields $\mathcal{B}_6$ with $J^P = 1/2^+$ and $\mathcal{B}_6^*$ with $J^P = 3/2^+$ in the 6_F flavor representation. The expressions for $H_a^{(\bar{Q})}$ and $\mathcal{S}_\mu$ read as

$$H_a^{(\bar{Q})} = [P_a^{*(\bar{Q})\mu}\gamma_\mu - P_a^{(\bar{Q})}\gamma_5]\frac{1-\not{v}}{2}, \tag{7}$$

$$\mathcal{S}_\mu = -\sqrt{\frac{1}{3}}(\gamma_\mu + v_\mu)\gamma^5\mathcal{B}_6 + \mathcal{B}_{6\mu}^*. \tag{8}$$

Here, $v = (1, \vec{0})$ is the four velocity under the non-relativistic approximation. $A_\mu = \frac{1}{2}(\xi^\dagger\partial_\mu\xi - \xi\partial_\mu\xi^\dagger)$ is the axial current, where $\xi = \exp(i\mathbb{P}/f_\pi)$ and $f_\pi = 132$ MeV is the pion decay constant. The matrices for $\mathbb{P}$, $\mathcal{B}_6$ and $\mathcal{B}_6^*$ are

$$\mathbb{P} = \begin{pmatrix} \frac{\pi^0}{\sqrt{2}} & \pi^+ \\ \pi^- & -\frac{\pi^0}{\sqrt{2}} \end{pmatrix}, \mathcal{B}_6 = \begin{pmatrix} \Sigma_c^{++} & \frac{\Sigma_c^+}{\sqrt{2}} \\ \frac{\Sigma_c^+}{\sqrt{2}} & \Sigma_c^0 \end{pmatrix}, \mathcal{B}_6^* = \begin{pmatrix} \Sigma_c^{*++} & \frac{\Sigma_c^{*+}}{\sqrt{2}} \\ \frac{\Sigma_c^{*+}}{\sqrt{2}} & \Sigma_c^{*0} \end{pmatrix}.$$

Substituting Eq. (7)-(8) into Eq. (5)-(6), we obtain

$$\mathcal{L}_{\bar{P}^*\bar{P}^*\mathbb{P}} = i\frac{2g}{f_\pi}v^\alpha\varepsilon_{\alpha\mu\nu\lambda}\bar{P}_a^{*\mu\dagger}\bar{P}_b^{*\lambda}\partial^\nu\mathbb{P}_{ab}, \tag{9}$$

$$\mathcal{L}_{\mathcal{B}_6\mathcal{B}_6\mathbb{P}} = i\frac{g_1}{2f_\pi}\varepsilon^{\mu\nu\lambda\kappa}v_\kappa \mathrm{Tr}\left[\bar{\mathcal{B}}_6\gamma_\mu\gamma_\lambda\partial_\nu\mathbb{P}\mathcal{B}_6\right], \tag{10}$$

$$\mathcal{L}_{\mathcal{B}_6^*\mathcal{B}_6^*\mathbb{P}} = -i\frac{3g_1}{2f_\pi}\varepsilon^{\mu\nu\lambda\kappa}v_\kappa \mathrm{Tr}\left[\bar{\mathcal{B}}_{6\mu}^*\partial_\nu\mathbb{P}\mathcal{B}_{6\nu}^*\right]. \tag{11}$$

Similar to the treatment in Ref. [38], the pionic coupling constant in Eq. (5) is determined as $g = 0.59 \pm 0.07 \pm 0.01$ from the D^* decay width. The coupling constant g_1 in Eq. (6) is fixed as $g_1 = 0.94$ [37].

By gauging the Wess-Zumino term, the vector-vector-pseudoscalar coupling was [39, 40],

$$\mathcal{L}_{\bar{K}^*\bar{K}^*\mathbb{P}} = -\sqrt{2}g_{\pi\bar{K}^*\bar{K}^*}\varepsilon^{\mu\nu\rho\sigma}\partial_\rho\bar{K}_\sigma^{*\dagger}\mathbb{P}\partial_\mu\bar{K}_\nu^*, \tag{12}$$

where $\bar{K}^*$ stands for $\bar{K}^* = (K^{*-}, \bar{K}^{*0})^T$. The coupling constant $g_{\pi\bar{K}^*\bar{K}^*}$ is determined as $g_{\pi\bar{K}^*\bar{K}^*} = \frac{g_2^2 N_c}{64\pi^2 f_\pi}$ with $N_c = 3$ and $g_2 = 13.7$.

We also need the normalization relations for the vector meson M^*, baryon $\mathcal{B}_6$ and $\mathcal{B}_6^{*\mu}$

$$\begin{aligned}
\langle 0|\bar{M}^*_\mu|\bar{Q}q(1^-)\rangle &= \epsilon_\mu\sqrt{M_{\bar{M}^*}}, \\
\langle 0|\mathcal{B}_6|Qqq(1/2^+)\rangle &= \sqrt{2M_{\mathcal{B}_6}}\left(\left(1-\frac{\vec{p}^2}{8M^2_{\mathcal{B}_6}}\right)\chi, \frac{\vec{\sigma}\cdot\vec{p}}{2M_{\mathcal{B}_6}}\chi\right)^T, \\
\langle 0|\mathcal{B}_6^{*\mu}|Qqq(3/2^+)\rangle &= \sum_{m_1,m_2} C^{3/2,m_1+m_2}_{1/2,m_1;1,m_2}\sqrt{2M_{\mathcal{B}^*_6}} \\
&\quad\times\left(\left(1-\frac{\vec{p}^2}{8M_{\mathcal{B}^*_6}}\right)\chi_{\frac{1}{2},m_1}, \frac{\vec{\sigma}\cdot\vec{p}}{2M_{\mathcal{B}^*_6}}\chi_{\frac{1}{2},m_1}\right)^T\epsilon^\mu_{m_2}.
\end{aligned}$$

2.3. Effective potential

In the OPE model, we first obtain the scattering amplitude in Fig. 2.

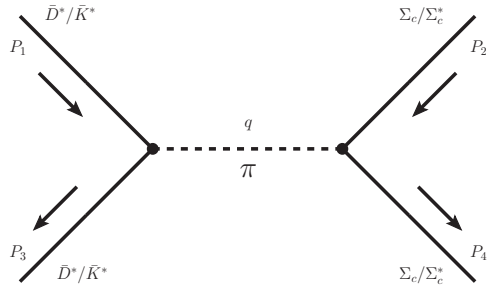

Figure 2: The Feynman diagrams for the $\Sigma_c\bar{D}^*$, $\Sigma_c^*\bar{D}^*$, $\Sigma_c\bar{K}^*$ and $\Sigma_c^*\bar{K}^*$ systems in OPE model.

The effective potential can be related to the scattering amplitude with the Breit approximation. For example, the effective potential for the $\Sigma_c\bar{D}^*$ system in the momentum space is

$$\mathcal{V}_E^{\Sigma_c\bar{D}^*\to\Sigma_c\bar{D}^*}(\vec{q}) = -\frac{\mathcal{M}(\Sigma_c\bar{D}^*\to\Sigma_c\bar{D}^*)}{\sqrt{\prod_i 2M_i\prod_f 2M_f}}, \tag{13}$$

where M_i and M_f are the masses of the initial and final states, respectively. $\mathcal{M}(\Sigma_c\bar{D}^*\to\Sigma_c\bar{D}^*)$ denotes the scattering amplitude for the $\Sigma_c\bar{D}^*\to\Sigma_c\bar{D}^*$ process by exchanging one pion meson in t-channel. The effective potential in the coordinate space $\mathcal{V}(\vec{r})$ is obtained by performing Fourier transformation

to the momentum space effective potential $\mathcal{V}(\vec{q})$,

$$\mathcal{V}_E^{\Sigma_c\bar{D}^*\leftrightarrow\Sigma_c\bar{D}^*}(\vec{r}) = \int \frac{d^3\vec{p}}{(2\pi)^3} e^{i\vec{p}\cdot\vec{(}r)} \mathcal{V}_E^{\Sigma_c\bar{D}^*\leftrightarrow\Sigma_c\bar{D}^*}(\vec{q}) \mathcal{F}^2(q^2, m_E^2).$$

In the above expression, the monopole form factor $\mathcal{F}(q^2, m_E^2)$ is introduced at each interaction vertex to compensate the off-shell effect of the exchanged pion. $\mathcal{F}(q^2, m_E^2) = (\Lambda^2 - m_E^2)/(\Lambda^2 - q^2)$, where m_E and q are the mass and four-momentum of the exchanged meson, respectively. Λ is the cutoff with the value around one to several GeV.

The general expressions of the subpotentials for the processes $\Sigma_c\bar{D}^* \to \Sigma_c\bar{D}^*$, $\Sigma_c^*\bar{D}^* \to \Sigma_c^*\bar{D}^*$, $\Sigma_c\bar{K}^* \to \Sigma_c\bar{K}^*$ and $\Sigma_c^*\bar{K}^* \to \Sigma_c^*\bar{K}^*$ are

$$\begin{aligned}
\mathcal{V}_\pi^{\Sigma_c\bar{D}^*\to\Sigma_c\bar{D}^*}(\vec{r}) &= \frac{gg_1}{f_\pi^2}\mathcal{V}_1, & (14)\\
\mathcal{V}_\pi^{\Sigma_c^*\bar{D}^*\to\Sigma_c^*\bar{D}^*}(\vec{r}) &= \frac{3}{2}\frac{gg_1}{f_\pi^2}\mathcal{V}_2, & (15)\\
\mathcal{V}_\pi^{\Sigma_c\bar{K}^*\to\Sigma_c\bar{K}^*}(\vec{r}) &= \frac{g_{\pi\bar{K}^*\bar{K}^*}g_1}{\sqrt{2}f_\pi}\mathcal{V}_1, & (16)\\
\mathcal{V}_\pi^{\Sigma_c^*\bar{K}^*\to\Sigma_c^*\bar{K}^*}(\vec{r}) &= \frac{3}{2\sqrt{2}}\frac{g_{\pi\bar{K}^*\bar{K}^*}g_1}{f_\pi}\mathcal{V}_2 & (17)
\end{aligned}$$

where

$$\begin{aligned}
\mathcal{V}_1 &= \frac{1}{3}\left[\left(i\vec{\epsilon_1}\times\vec{\epsilon_3}^\dagger\right)\cdot\vec{\sigma}\right]\nabla^2 Y(\Lambda, m_\pi, \vec{r})\\
&\quad + \frac{1}{3}S(\hat{r}, i\vec{\epsilon_1}\times\vec{\epsilon_3}^\dagger, \vec{\sigma}) r\frac{\partial}{\partial r}\frac{1}{r}\frac{\partial}{\partial r}Y(\Lambda, m_\pi, \vec{r}), & (18)\\
\mathcal{V}_2 &= \sum_{a,b,c,d}\left\langle\frac{1}{2}, a; 1, b\middle|\frac{3}{2}, a+b\right\rangle\left\langle\frac{1}{2}, c; 1, d\middle|\frac{3}{2}, c+d\right\rangle\chi_4^{a\dagger}\chi_2^c\\
&\quad \times\Big\{\frac{1}{3}\left(\vec{\epsilon}_1\times\vec{\epsilon}_3^\dagger\right)\cdot\left(\vec{\epsilon}_2^{\,d}\times\vec{\epsilon}_4^{\,b\dagger}\right)\nabla^2 Y(\Lambda, m_\pi, \vec{r})\\
&\quad + \frac{1}{3}S\left(\hat{r}, \vec{\epsilon}_1\times\vec{\epsilon}_3^\dagger, \vec{\epsilon}_2^{\,d}\times\vec{\epsilon}_4^{\,b\dagger}\right) r\frac{\partial}{\partial r}\frac{1}{r}\frac{\partial}{\partial r}Y(\Lambda, m_\pi, \vec{r})\Big\}. & (19)
\end{aligned}$$

In the above expressions, $S(\hat{r}, \vec{x}, \vec{y}) = 3(\hat{r}\cdot\vec{x})(\hat{r}\cdot\vec{y}) - \vec{x}\cdot\vec{y}$, and

$$Y(\Lambda, m, r) = \frac{1}{4\pi r}(e^{-mr} - e^{-\Lambda r}) - \frac{\Lambda^2 - m^2}{8\pi\Lambda}e^{-\Lambda r}. \quad (20)$$

To obtain the total effective potentials of the $\Sigma_c\bar{M}^*$ and $\Sigma_c^*\bar{M}^*$ systems, the effective potentials in Eqs. (14)-(17) should be sandwiched between the flavor wave functions. Thus, the general total effective potential for different systems can be expressed as

$$V_{\rm total}^{\Sigma_c\bar{M}^*} = \mathcal{G}\mathcal{V}_\pi^{\Sigma_c\bar{M}^*\to\Sigma_c\bar{M}^*}(\vec{r}), \tag{21}$$

$$V_{\rm total}^{\Sigma_c^*\bar{M}^*} = -\mathcal{G}\mathcal{V}_\pi^{\Sigma_c^*\bar{M}^*\to\Sigma_c^*\bar{M}^*}(\vec{r}), \tag{22}$$

where the isospin factor $\mathcal{G}=1$ for the isospin-1/2 system and $\mathcal{G}=-1/2$ for the isospin-3/2 system. The angular momentum operators in Eqs. (14)-(17) will be replaced by a series of numerical matrixes collected in Table 1. We need to specify that the S-D mixing effect is considered in our calculation, which makes the corresponding replacements in Eqs. (18)-(20) just indicated in Table 1.

Table 1: The matrix expressions for the angular momentum operators according to $\langle^{2S'+1}L'_{J'}|\Omega_i|^{2S+1}L_J\rangle$. Here, $\Omega_1 = (i\vec{\epsilon}_1\times\vec{\epsilon}_3^{\,\dagger})\cdot\vec{\sigma}$, $\Omega_2 = S(\hat{r}, i\vec{\epsilon}_1\times\vec{\epsilon}_3^{\,\dagger},\vec{\sigma})$, $\Omega_3 = \sum_{a,b;c,d} C^{3/2,m}_{1/2,a;1,b}C^{3/2,n}_{1/2,c;1,d}\chi_4^{a\dagger}\chi_2^c(\vec{\epsilon}_1\times\vec{\epsilon}_3^{\,\dagger})\cdot(\vec{\epsilon}_2^{\,d}\times\vec{\epsilon}_2^{\,b\dagger})$ and $\Omega_4 = \sum_{a,b;c,d} C^{3/2,m}_{1/2,a;1,b}C^{3/2,n}_{1/2,c;1,d}\chi_4^{a\dagger}\chi_2^c S(\hat{r},\vec{\epsilon}_1\times\vec{\epsilon}_3^{\,\dagger},\vec{\epsilon}_2^{\,d}\times\vec{\epsilon}_2^{\,b\dagger})$.

J	$1/2$	$3/2$	$5/2$
Ω_1	$\begin{pmatrix} -2 & 0 \\ 0 & 1 \end{pmatrix}$	$\begin{pmatrix} 1 & 0 & 0 \\ 0 & -2 & 0 \\ 0 & 0 & 1 \end{pmatrix}$	$\times$
Ω_2	$\begin{pmatrix} 0 & -\sqrt{2} \\ -\sqrt{2} & -2 \end{pmatrix}$	$\begin{pmatrix} 0 & 1 & 2 \\ 1 & 0 & -1 \\ 2 & -1 & 0 \end{pmatrix}$	$\times$
Ω_3	$\begin{pmatrix} \frac{5}{3} & 0 \\ 0 & \frac{2}{3} \end{pmatrix}$	$\begin{pmatrix} \frac{2}{3} & 0 & 0 \\ 0 & \frac{5}{3} & 0 \\ 0 & 0 & \frac{2}{3} \end{pmatrix}$	$\begin{pmatrix} -1 & 0 & 0 & 0 \\ 0 & \frac{5}{3} & 0 & 0 \\ 0 & 0 & \frac{2}{3} & 0 \\ 0 & 0 & 0 & -1 \end{pmatrix}$
Ω_4	$\begin{pmatrix} 0 & -\frac{7}{3\sqrt{5}} \\ -\frac{7}{3\sqrt{5}} & \frac{16}{15} \end{pmatrix}$	$\begin{pmatrix} 0 & \frac{7}{3\sqrt{10}} & -\frac{16}{15} \\ \frac{7}{3\sqrt{10}} & 0 & -\frac{7}{3\sqrt{10}} \\ -\frac{16}{15} & -\frac{7}{3\sqrt{10}} & 0 \end{pmatrix}$	$\begin{pmatrix} 0 & \frac{2}{\sqrt{15}} & \frac{1}{5}\sqrt{\frac{3}{7}} & -\frac{2\sqrt{14}}{5} \\ \frac{2}{\sqrt{15}} & 0 & \frac{1}{3}\sqrt{\frac{7}{5}} & -4\sqrt{\frac{2}{105}} \\ \frac{1}{5}\sqrt{\frac{3}{7}} & \frac{1}{3}\sqrt{\frac{7}{5}} & -\frac{16}{21} & -\frac{1}{7}\sqrt{\frac{2}{3}} \\ -\frac{2\sqrt{14}}{5} & -4\sqrt{\frac{2}{105}} & -\frac{1}{7}\sqrt{\frac{2}{3}} & -\frac{4}{7} \end{pmatrix}$

3. Numerical results

With the obtained OPE effective potentials for the $\Sigma_c\bar{M}^*$ and $\Sigma_c^*\bar{M}^*$ systems with $\bar{M}^* = (\bar{D}^*, \bar{K}^*)$ listed in Section 2, we can find the possible

bound solutions (the binding energy E, corresponding root-mean-square radius r_{RMS} and radial wave function $\phi(r)$) by solving the coupled-channel Schrödinger equation with the help of the FESSDE program [41, 42]. The corresponding kinetic terms include

$$K^{J=1/2}_{\Sigma_c\bar{M}^*} = \text{diag}\left(-\frac{1}{2m_1}\nabla^2, -\frac{1}{2m_1}\nabla_1^2\right), \quad (23)$$

$$K^{J=3/2}_{\Sigma_c\bar{M}^*} = \text{diag}\left(-\frac{1}{2m_1}\nabla^2, -\frac{1}{2m_1}\nabla_1^2, -\frac{1}{2m_1}\nabla_1^2\right), \quad (24)$$

$$K^{J=1/2}_{\Sigma_c^*\bar{M}^*} = \text{diag}\left(-\frac{1}{2m_2}\nabla^2, -\frac{1}{2m_2}\nabla_1^2\right), \quad (25)$$

$$K^{J=3/2}_{\Sigma_c^*\bar{M}^*} = \text{diag}\left(-\frac{1}{2m_2}\nabla^2, -\frac{1}{2m_2}\nabla_1^2, -\frac{1}{2m_2}\nabla_1^2\right), \quad (26)$$

$$K^{J=3/2}_{\Sigma_c^*\bar{M}^*} = \text{diag}\left(-\frac{1}{2m_2}\nabla^2, -\frac{1}{2m_2}\nabla_1^2, -\frac{1}{2m_2}\nabla_1^2, -\frac{1}{2m_2}\nabla_1^2\right) \quad (27)$$

with $\nabla^2 = \frac{1}{r^2}\frac{\partial}{\partial r}r^2\frac{\partial}{\partial r}$ and $\nabla_1^2 = \nabla^2 - 6/r^2$, where m_1 and m_2 are the reduced masses of the $\Sigma_c\bar{M}^*$ and $\Sigma_c^*\bar{M}^*$ system, respectively.

3.1. $P_c(4380)$ *and* $P_c(4450)$

In Ref. [11], the authors considered the S-wave contribution only and obtained the bound solutions for the systems $\Sigma_c\bar{D}^*$ with $(I = 1/2, J^P = 3/2^-)$ and $\Sigma_c^*\bar{D}^*$ with $(I = 1/2, J^P = 5/2^-)$, which may correspond to $P_c(4380)$ and $P_c(4450)$, respectively. In this work, we include the S-D mixing and restudy these systems. The numerical results for the $\Sigma_c\bar{D}^*$ system with $(I = 1/2, J^P = 3/2^-)$ and the $\Sigma_c^*\bar{D}^*$ system with $(I = 1/2, J^P = 5/2^-)$ are shown in Fig. 3. For comparison, we also present the results with the S-wave contribution only in Fig. 3.

We compare the total effective potentials with and without the S-D mixing effect in Fig. 3 (a) and (I). With the S-D mixing effect, the spatial wave functions for the $\Sigma_c\bar{D}^*$ system with $(I = 1/2, J^P = 3/2^-)$ is a $[3\times 1]$ column vector with $(|\phi_S\rangle, |\phi_{D1}\rangle, |\phi_{D2}\rangle)^T$. As shown in Fig. 3 (b), the dash lines with different color stand for the spatial wave functions $|\phi_{^4\mathbb{S}_{\frac{3}{2}}}\rangle$, $|\phi_{^2\mathbb{D}_{\frac{3}{2}}}\rangle$ and $|\phi_{^4\mathbb{D}_{\frac{3}{2}}}\rangle$, which are abbreviated as ϕ_S, ϕ_{D1} and ϕ_{D2} in Fig. 3 (b). The probability for each component is $\int|\phi_i|^2dr/\sum_i\int|\phi_i|^2dr$. The S-wave contribution is dominant and plays a major role in the formation of molecular pentaquarks.

We notice that the masses of $P_c(4380)$ and $P_c(4450)$ can be reproduced well under the $\Sigma_c\bar{D}^*$ with $(I = 1/2, J^P = 3/2^-)$ and $\Sigma_c^*\bar{D}^*$ with $(I = 1/2, J^P = 5/2^-)$ molecular assignments, respectively (see Fig. 3 (a) and (I)). In Fig. 3, the red solid curves stand for the obtained bound state solutions (effective potentials V [MeV] and radial wave functions $\phi(r)$ [fm$^{-1/2}$]) if only considering the S-wave effect. In this case, $\Lambda = 2.35$ GeV and $\Lambda = 1.77$ GeV are taken for the $\Sigma_c\bar{D}^*$ and $\Sigma_c^*\bar{D}^*$ systems, respectively. The dashed blue curves are the corresponding effective potentials and radial wave functions for the $\Sigma_c\bar{D}^*$ system with $(I = 1/2, J^P = 3/2^-)$ and the $\Sigma_c^*\bar{D}^*$ system with $(I = 1/2, J^P = 5/2^-)$. Now, the cutoff $\Lambda = 1.78$ GeV and $\Lambda = 1.54$ GeV are taken for the $\Sigma_c\bar{D}^*$ system with $(I = 1/2, J^P = 3/2^-)$ and the $\Sigma_c^*\bar{D}^*$ system with $(I = 1/2, J^P = 5/2^-)$, respectively, in order to reproduce the masses of $P_c(4380)$ and $P_c(4450)$. After comparing the results with and without the S-D mixing effect, we find that the cutoff values become smaller with the S-D mixing effect. In other words, the S-D mixing effect is indeed helpful to the formation of these bound states.

We also notice that there exists slight difference of the fitted Λ values for the $\Sigma_c\bar{D}^*$ and $\Sigma_c^*\bar{D}^*$, which are used to reproduce the central values of masses of $P_c(4380)$ and $P_c(4450)$. If considering the experimental errors for their mass measurement, the difference of the fitted Λ values for the $\Sigma_c\bar{D}^*$ and $\Sigma_c^*\bar{D}^*$ becomes subtle.

Under the S-wave hidden-charm molecular state assignment to $P_c(4380)$ and $P_c(4450)$, the parities of $P_c(4380)$ and $P_c(4450)$ are negative. However, the LHCb's measurement suggests that $P_c(4380)$ and $P_c(4450)$ have opposite parities [2]. Facing such situation, we need to clarify this point. Under the molecular state scheme, there may also exist the P-wave, D-wave or even higher orbital excitations if the binding energy of the lowest S-wave hadronic molecule reaches up to several tens of MeV. The P-wave state has an excitation energy around several to tens of MeV, which is slightly higher than that of the S-wave ground state. Considering this status, there exists the possibility that the S-wave and P-wave states may completely overlap with each other, i.e., two or more resonant signals around 4450 MeV may exist, where these two states are close to each other but may carry different parity. If the P-wave or higher excitation is very broad, such a state may easily be mistaken as the background.

While the observed $P_c(4380)$ corresponds to the discussed S-wave $\Sigma_c\bar{D}^*$ molecular state, the observed $P_c(4450)$ may be a P-wave excitation. There may also exist a very broad S-wave $\Sigma_c^*\bar{D}^*$ molecular state around 4450 MeV

which was discussed in the present work. This broad S-wave state around 4450 MeV cannot be distinguished from the background. The fact that the different assignment of the spin and parity of these two P_c states yields roughly the same good fit [11] can be reasonably understood.

On the other hand, if the P-wave excitation lies several MeV within 4380 MeV and has a width as narrow as several MeV, it will be hard to identify this state since it may probably be buried by the broad $P_c(4380)$ resonance with 205 MeV width. Thus, we also suggest future experiment to collect a huge amount of experimental data to identify the nearly degenerate resonances with different parities and widths.

3.2. Other hidden-charm molecular pentaquarks

Besides $P_c(4380)$ and $P_c(4450)$, we further predict other possible hidden-charm $\Sigma_c^{(*)}\bar{D}^*$ molecular pentaquarks and collect the corresponding results in Table 2. Our numerical results are rather sensitive to the cutoff parameter Λ. In this work, we present the bound state solutions by scanning a $\Lambda < 5$ GeV range from the experience of the nuclear force [43, 44, 45, 46].

Table 2: The typical values of the obtained bound state solutions $[\Lambda, E, r_{RMS}]$ for the hidden-charm $\Sigma_c\bar{D}^*$ and $\Sigma_c^*\bar{D}^*$ systems with all possible configurations and (I, J^P) quantum numbers. Here, E, r_{RMS}, and Λ are in units of MeV, fm, and GeV, respectively. The masses of these discussed molecular states can be determined by relation $M_{the} + E$. Here, threshold energy M_{the} is taken as 4462 MeV and 4527 MeV for the $\Sigma_c\bar{D}^*$ and $\Sigma_c^*\bar{D}^*$ systems, respectively.

$\Sigma_c\bar{D}^*$		$\Sigma_c^*\bar{D}^*$		
$(1/2, 1/2^-)$		$(1/2, 1/2^-)$	$(1/2, 3/2^-)$	
$[2.53, -2.42, 2.26]$		$[2.72, -2.43, 2.31]$	$[2.18, -2.48, 2.26]$	
$[2.65, -7.58, 1.38]$		$[2.92, -8.73, 1.35]$	$[2.38, -9.10, 1.33]$	
$(I, J^P) = (3/2, 1/2^-)$	$(3/2, 3/2^-)$	$(3/2, 1/2^-)$	$(3/2, 3/2^-)$	$(3/2, 5/2^-)$
$[1.73, -2.55, 1.95]$	$[4.16, -2.27, 2.20]$	$[1.44, -2.65, 1.92]$	$[2.36, -1.80, 2.33]$	$[3.76, -2.54, 2.11]$
$[1.85, -8.91, 1.10]$	$[4.38, -7.06, 1.32]$	$[1.56, -9.81, 1.07]$	$[2.56, -9.78, 1.08]$	$[3.96, -7.48, 1.32]$

If the cutoff is allowed to vary in the range $0.5 \sim 5$ GeV, there exist bound solutions for the $\Sigma_c\bar{D}^*$ systems with $(I, J^P) = (1/2, 1/2^-)$, $(1/2, 3/2^-)$, $(3/2, 1/2^-)$ and $(3/2, 3/2^-)$, and the $\Sigma_c^*\bar{D}^*$ systems with $(I, J^P) = (1/2, 1/2^-)$, $(1/2, 3/2^-)$, $(1/2, 5/2^-)$, $(3/2, 1/2^-)$, $(3/2, 3/2^-)$ and $(3/2, 5/2^-)$.

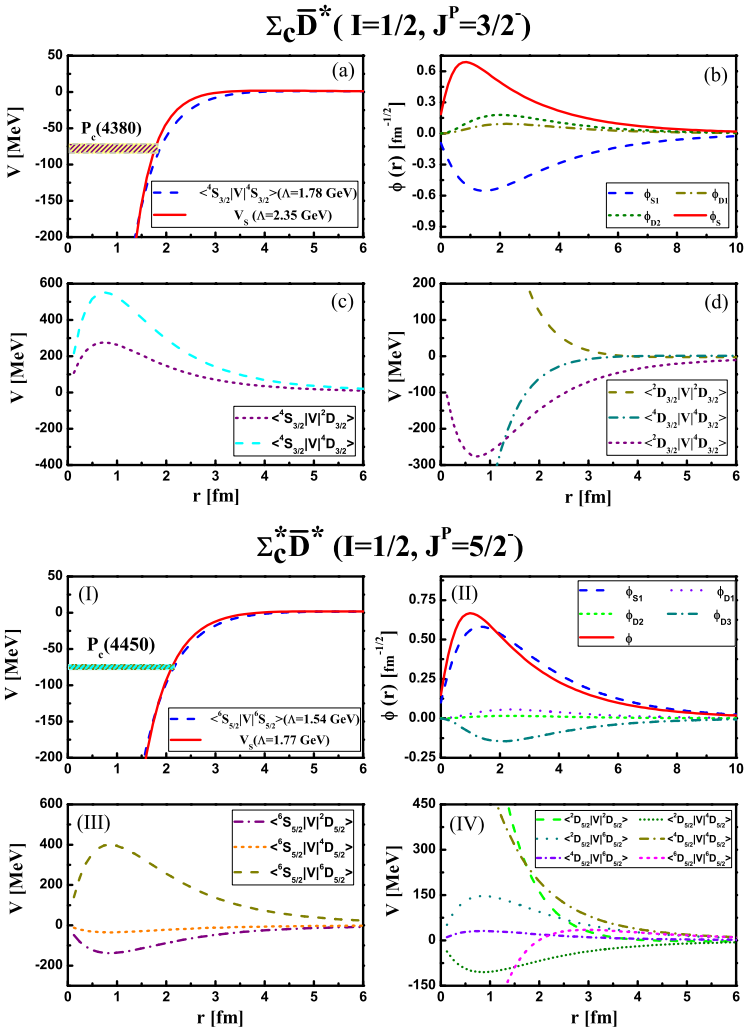

Figure 3: (color online). The variations of the obtained OPE effective potentials with r for the $\Sigma_c^{(*)}\bar{D}^*$ systems, and the obtained bound state solutions. Here, ϕ_{S1}, ϕ_{D1} and ϕ_{D2} in Fig. 3 (b) denote the spatial wave functions of the $\Sigma_c\bar{D}^*$ ($I = 1/2$, $J^P = 3/2^-$) state with the angular wave functions $|^4\mathbb{S}_{\frac{3}{2}}\rangle$, $|^2\mathbb{D}_{\frac{3}{2}}\rangle$ and $|^4\mathbb{D}_{\frac{3}{2}}\rangle$, respectively. The notations ϕ_S, ϕ_{D1}, ϕ_{D2} and ϕ_{D3} in Fig. 3 (II) are the same as in Fig. 3 (b).

If the cutoff is fixed as $\Lambda = 1.78$ GeV in order to reproduce the mass of $P_c(4380)$ under the $\Sigma_c\bar{D}^*$ $(I = 1/2, J^P = 3/2^-)$ assignment, there exists a shallow $\Sigma_c\bar{D}^*$ $(I = 3/2, J^P = 1/2^-)$ molecular state, which is marked as $P_c'(4460)$ in Table 2, where the obtained energy is $E \simeq -5$ MeV. For the $\Sigma_c^*\bar{D}^*$ system, we find the bound state solution ($E \simeq -10$ MeV) for the $\Sigma_c^*\bar{D}^*$ system with $(I = 3/2, J^P = 1/2^-)$ with the cutoff $\Lambda = 1.54$ GeV which is adopted to reproduce the mass of $P_c(4450)$. This state is named as $P_c'(4520)$.

With $\Lambda = 1.78$ GeV for the $\Sigma_c\bar{D}^*$ systems and $\Lambda = 1.54$ GeV for the $\Sigma_c^*\bar{D}^*$ systems, we cannot find a bound state solution for the $\Sigma_c\bar{D}^*$ systems with $(I, J^P) = (1/2, 1/2^-)$ and $(3/2, 3/2^-)$, the $\Sigma_c^*\bar{D}^*$ systems with $(I, J^P) = (1/2, 1/2^-), (1/2, 3/2^-), (3/2, 3/2^-)$ and $(3/2, 5/2^-)$. This observation is almost the same as in Ref. [11] where only the S-wave is taken into account .

In short summary, there exist at least two hidden-charm shallow molecular pentaquarks $P_c'(4460)$ and $P_c'(4520)$, which are the partners of $P_c(4380)$ and $P_c(4450)$. In Table 3, we list these allowed decay modes of $P_c(4380)$, $P_c(4450)$, $P_c'(4460)$ and $P_c'(4520)$.

Table 3: The allowed decay channels for $P_c(4380)$, $P_c(4450)$, $P_c'(4460)$ and $P_c'(4520)$. Here, S and D stand for the S-wave and D-wave decay mode, respectively. And $\times$ indicates that this decay process is forbidden.

Decay channels	$\Sigma_c\bar{D}^*(1/2, 3/2^-)$	$\Sigma_c\bar{D}^*(3/2, 1/2^-)$	$\Sigma_c^*\bar{D}^*(1/2, 5/2^-)$	$\Sigma_c^*\bar{D}^*(3/2, 1/2^-)$
$\Lambda_c\bar{D}$	D	$\times$	D	$\times$
$\Lambda_c\bar{D}^*$	S/D	$\times$	D	$\times$
$\Sigma_c\bar{D}$	D	$\times$	D	$\times$
$\eta_c N$	D	$\times$	D	$\times$
$J/\psi N$	S	$\times$	D	$\times$
$\eta_c\Delta$	D	S	D	S
$J/\psi\Delta$	S	S	D	S

3.3. Charm-strange molecular pentaquarks

The numerical results of the $\Sigma_c\bar{K}^*$ and $\Sigma_c^*\bar{K}^*$ systems with all possible quantum numbers are listed in Table 4, where the cutoff is allowed to vary in the range $\Lambda = 0.5 \sim 5$ GeV. There exist bound state solutions for the $\Sigma_c\bar{K}^*$ systems with $(I = 1/2, J^P = 1/2^-)$ and $(I = 3/2, J^P = 1/2^-)$, and the $\Sigma_c^*\bar{K}^*$

Table 4: The typical values of the obtained bound state solutions $[\Lambda, E, r_{RMS}]$ for the $\Sigma_c\bar{K}^*$ and $\Sigma_c^*\bar{K}^*$ systems. Here, E, r_{RMS}, and Λ are in units of MeV, fm, and GeV, respectively. And $[\times]$ indicates that there does not exist a bound state solution. The masses of these discussed molecular states can be determined by relation $M_{the}+E$. Here, threshold energy M_{the} is taken as 3345 MeV and 3410 MeV for the $\Sigma_c\bar{K}^*$ and $\Sigma_c^*\bar{K}^*$ systems, respectively.

$\Sigma_c\bar{K}^*$		$\Sigma_c^*\bar{K}^*$		
$(I, J^P) = (1/2, 1/2^-)$	$(1/2, 3/2^-)$	$(1/2, 1/2^-)$	$(1/2, 3/2^-)$	$(1/2, 5/2^-)$
$[3.84, -2.24, 2.83]$	$[1.78, -3.88, 2.16]$	$[4.14, -2.13, 2.94]$	$[3.22, -2.11, 2.91]$	$[1.05, -2.43, 2.16]$
$[3.98, -9.58, 1.46]$	$[1.84, -7.31, 1.63]$	$[4.34, -9.18, 1.52]$	$[3.42, -9.24, 1.52]$	$[1.17, -9.66, 1.22]$
$(I, J^P) = (3/2, 1/2^-)$	$(3/2, 3/2^-)$	$(3/2, 1/2^-)$	$(3/2, 3/2^-)$	$(3/2, 5/2^-)$
$[2.52, -2.20, 2.63]$	$[\times]$	$[2.08, -2.63, 2.43]$	$[3.56, -2.49, 2.51]$	$[\times]$
$[2.62, -7.77, 1.45]$	$[\times]$	$[2.18, -9.09, 1.36]$	$[3.70, -9.04, 1.37]$	$[\times]$

systems with $(I = 1/2, J^P = 1/2^-)$, $(I = 1/2, J^P = 3/2^-)$, $(I = 3/2, J^P = 1/2^-)$ and $(I = 3/2, J^P = 3/2^-)$.

If we take $\Lambda = 1.77$ GeV for the $\Sigma_c\bar{K}^*$ systems and Λ =1.54 GeV for the $\Sigma_c^*\bar{K}^*$ systems from the experience of $P_c(4380)$ and $P_c(4450)$, there only exist two charm-strange molecular pentaquarks $P_{cs}(3340)$ and $P_{cs}(3400)$ corresponding to the $\Sigma_c\bar{K}^*$ $(I = 1/2, J^P = 3/2^-)$ molecular pentaquark with $E_{bin} = -3.88$ MeV and the $\Sigma_c^*\bar{K}^*$ $(I = 1/2, J^P = 5/2^-)$ system with $E_{bin} = -6.94$ MeV, respectively. We denote these two charm-strange molecular pentaquarks as $P_{cs}(3340)$ and $P_{cs}(3400)$, where the numbers 3340 MeV and 3400 MeV are their mass deduced from the relations $m_{\Sigma_c} + m_{\bar{K}^*} + E_{bin}$ and $m_{\Sigma_c^*} + m_{\bar{K}^*} + E_{bin}$, respectively. In other words, we adopt their masses to name these two predicted charm-strange molecular pentaquarks. The possible decay channels of $P_{cs}(3340)(I = 1/2, J^P = 3/2^-)$ and $P_{cs}(3400)(I = 1/2, J^P = 5/2^-)$ are shown in Table 5. As shown in Fig. 1 (b), $P_{cs}(3340)$ and $P_{cs}(3400)$ can be produced via the $\Lambda_b \to \bar{D}^0 P_{cs}^0$ decay at LHCb.

In the search of the charm-strange molecular pentaquarks $P_{cs}(3340)$ and $P_{cs}(3400)$, it is important to distinguish $P_{cs}(3340)$ and $P_{cs}(3400)$ from the excited P-wave charm-strange baryons $\Xi_c(1P, 2P)$ etc. The charm-strange baryon $\Xi_c(3123)$ was observed by the BABAR Collaboration [47]. Its mass is around 220-280 MeV lower than $P_{cs}(3340)$ and $P_{cs}(3400)$.

In the relativistic quark-diquark picture, Ebert *et al.* predicted the masses

Table 5: The allowed decay channels of $P_{cs}(3340)(I = 1/2, J^P = 3/2^-)$ and $P_{cs}(3400)(I = 1/2, J^P = 5/2^-)$. The S, P, D and F denote the S-wave, P-wave, D-wave and F-wave decay modes respectively.

	$D\Lambda$	$D\Lambda(1405)$	$D\Lambda(1520)$	$D\Sigma$	$D\Sigma(1385)$	$D\Sigma(1660)$	$D^*\Lambda/\Sigma$
$P_{cs}(3340)$	D	P	P	D	S	D	S
$P_{cs}(3400)$	D	F	P	D	D	D	D
	$\bar{K}\Lambda_c$	$\bar{K}\Lambda_c(2595)$	$\bar{K}\Lambda_c(2625)$	$\bar{K}\Sigma_c$	$\bar{K}\Sigma_c^*$		
$P_{cs}(3340)$	D	P	P	D	S		
$P_{cs}(3400)$	D	F	P	D	D		
	$\Xi_c\pi/\eta$	$\Xi_c\rho/\omega$	$\Xi_c'\pi/\eta$		$\Xi_c(2645)\pi/\eta$	$\Xi_c(2790)\pi$	$\Xi_c(2815)\pi$
$P_{cs}(3340)$	D	S	D		S	P	P
$P_{cs}(3400)$	D	D	D		D	F	P

of the charm-strange baryons [48]. The mass of $\Xi_c(2P)$ with the scalar diquark $S_{qq} = 0$ and $(I = 1/2, J^P = 3/2^-)$ is 3199 MeV. For the $(I = 1/2, J^P = 5/2^-)$ Ξ_c state with the vector diquark $S_{qq} = 1$, the 1P and 2P masses are 2921 MeV and 3282 MeV for $2P$ state respectively. Fortunately, the above two charmed baryons predicted in Ref. [48] do not overlap with $P_{cs}(3340)$ and $P_{cs}(3400)$.

However, the mass of the $(I = 1/2, J^P = 5/2^-)$ $\Xi_c(1F)$ charm-strange baryon with $S_{qq} = 1$ was predicted to be around 3.4 GeV [48], which overlaps with the $P_{cs}(3400)$. In this case, the experimental identification of the $P_{cs}(3400)$ signal will be very challenging. The overpopulation of the the $(I = 1/2, J^P = 5/2^-)$ charm-strange baryon around 3400 MeV may provide some hints. On the other hand, the 1F charm-strange baryon and $P_{cs}(3400)$ may have very different decay patterns because of their different internal structures. Further experimental and theoretical efforts will be helpful to search for the charm-strange molecular pentaquarks.

3.4. Hidden-bottom and B_c-like molecular pentaquarks

In Ref. [49], Wu and Zou once predicted the hidden-bottom pentaquark states. where they adopted the meson-baryon coupled channel unitary approach with the local hidden gauge formalism.

In the present work, we extend the obtained OPE effective potentials to

study the hidden-bottom $\Sigma_b^{(*)}B^*$ and B_c-like $\Sigma_b^{(*)}\bar{D}^*$ and $\Sigma_c^{(*)}B^*$ molecular pentaquarks. The reduced masses of the hidden-bottom and B_c-like molecular systems are heavier than those of the hidden-charm molecular system. Hence the kinetic energies of the hidden-bottom and B_c-like molecular pentaquark systems are significantly smaller than those of the hidden-charm molecular pentaquark system. Therefore, the hidden-bottom and B_c-like molecular systems are bound more tightly than the hidden-charm molecular systems. We collect the bound state solutions of the hidden-bottom and B_c-like molecular pentaquark systems in Table 6.

For the $\Sigma_b B^*$, $\Sigma_c B^*$, $\Sigma_b \bar{D}^*$ and $\Sigma_c \bar{D}^*$ systems with the same (I, J^P) quantum number, the corresponding cutoff values satisfy the relation $\Lambda_{\Sigma_b B^*} < \Lambda_{\Sigma_c B^*} < \Lambda_{\Sigma_b \bar{D}^*} < \Lambda_{\Sigma_c \bar{D}^*}$ if we require the same binding energy. Similarly, we have $\Lambda_{\Sigma_b^* B^*} < \Lambda_{\Sigma_c^* B^*} < \Lambda_{\Sigma_b^* \bar{D}^*} < \Lambda_{\Sigma_c^* \bar{D}^*}$ for the $\Sigma_b^* B^*$, $\Sigma_c^* B^*$, $\Sigma_b^* \bar{D}^*$ and $\Sigma_c^* \bar{D}^*$ systems with the same (I, J^P) quantum number and the same binding energy. In Table 7, we list the allowed decay modes of these hidden-bottom and B_c-like molecular pentaquarks.

We need to emphasize that several states with the same quantum numbers and very small binding energy appear (see Table 6). If assuming that these states would have a width similar to that of the two observed P_c states so far experimentally, the mass gap between these bound states would be much smaller than their widths. Thus, it might be hard to identify them experimentally.

4. Summary

Inspired by the observation of $P_c(4380)$ and $P_c(4450)$ by LHCb [2], we have investigated the possible molecular pentaquarks composed of a charmed baryon (Σ_c, Σ_c^*) and a $\bar{D}^*$ meson in the framework of the OPE model, where the S-D mixing effect is included in our calculation. Our result indicates the $\Sigma_c \bar{D}^*$ molecular state with $(I = 1/2, J^P = 3/2^-)$ and the $\Sigma_c^* \bar{D}^*$ molecular state with $(I = 1/2, J^P = 5/2^-)$ have the same mass range as that of the observed $P_c(4380)$ and $P_c(4450)$, respectively. We also predict their two partner states composed of the $\Sigma_c \bar{D}^*$ with $(I = 3/2, J^P = 1/2^-)$ and $\Sigma_c^* \bar{D}^*$ with $(I = 3/2, J^P = 1/2^-)$. We extend the same formalism and predict the hidden-bottom/B_c-like molecular pentaquarks and discuss their strong decay modes.

As a byproduct, we have also studied the charm-strange molecular pentaquarks composed of a charmed baryon (Σ_c, Σ_c^*) and a $\bar{K}^*$ meson. We pre-

Table 6: The obtained bound state solutions $[\Lambda, E, r_{RMS}]$ for the hidden-bottom and B_c-like molecular pentaquark systems. Here, E, r_{RMS}, and Λ are in units of MeV, fm, and GeV, respectively. The masses of these discussed molecular states can be determined by relation $M_{the} + E$. Here, threshold energy M_{the} is taken as 11139 MeV, 7779 MeV, 7822 MeV, 11159 MeV, 7843 MeV and 7842 MeV for the $\Sigma_b B^*$, $\Sigma_c B^*$, $\Sigma_b \bar{D}^*$, $\Sigma_b^* B^*$, $\Sigma_c^* B^*$, $\Sigma_b^* \bar{D}^*$ systems, respectively.

(I, J^P)	$\Sigma_b B^*$	$\Sigma_c B^*$	$\Sigma_b \bar{D}^*$
$(1/2, 1/2^-)$	$[1.21, -2.39, 1.84]$	$[1.78, -2.67, 1.93]$	$[1.95, -2.38, 2.09]$
	$[1.36, -9.09, 1.14]$	$[1.93, -9.69, 1.17]$	$[2.10, -9.07, 1.22]$
$(1/2, 3/2^-)$	$[0.72, -2.63, 1.65]$	$[0.94, -2.39, 1.94]$	$[1.02, -2.68, 1.92]$
	$[0.84, -8.91, 1.05]$	$[1.06, -8.32, 1.19]$	$[1.14, -8.92, 1.19]$
$(3/2, 1/2^-)$	$[0.92, -2.72, 1.35]$	$[1.25, -2.08, 1.81]$	$[1.37, -2.36, 1.79]$
	$[1.04, -8.72, 0.84]$	$[1.40, -9.58, 0.93]$	$[1.49, -8.21, 1.03]$
$(3/2, 3/2^-)$	$[2.01, -2.81, 1.54]$	$[2.90, -2.22, 1.93]$	$[3.20, -2.22, 2.00]$
	$[2.31, -9.89, 0.95]$	$[3.20, -8.83, 1.08]$	$[3.50, -8.99, 1.10]$
(I, J^P)	$\Sigma_b^* B^*$	$\Sigma_c^* B^*$	$\Sigma_b^* \bar{D}^*$
$(1/2, 1/2^-)$	$[1.32, -2.40, 1.92]$	$[1.90, -2.47, 2.06]$	$[2.11, -2.27, 2.20]$
	$[1.53, -8.80, 1.22]$	$[2.10, -8.49, 1.28]$	$[2.35, -9.88, 1.22]$
$(1/2, 3/2^-)$	$[1.15, -2.80, 1.80]$	$[1.55, -2.11, 2.17]$	$[1.37, -2.51, 2.16]$
	$[1.35, -9.55, 1.18]$	$[1.75, -2.00, 1.30]$	$[1.58, -9.63, 1.32]$
$(1/2, 5/2^-)$	$[0.62, -2.13, 1.74]$	$[0.80, -2.17, 1.98]$	$[0.86, -1.95, 2.15]$
	$[0.74, -9.12, 1.00]$	$[0.92, -9.04, 1.12]$	$[0.98, -8.54, 1.19]$
$(3/2, 1/2^-)$	$[0.79, -2.43, 1.44]$	$[1.05, -2.07, 1.82]$	$[1.15, -2.02, 1.94]$
	$[0.91, -8.98, 0.85]$	$[1.15, -6.89, 1.08]$	$[1.27, -8.23, 1.05]$
$(3/2, 3/2^-)$	$[1.20, -2.10, 1.56]$	$[1.70, -2.35, 1.75]$	$[1.90, -2.75, 1.71]$
	$[1.40, -9.65, 0.84]$	$[1.85, -7.79, 1.04]$	$[2.05, -8.70, 1.04]$
$(3/2, 5/2^-)$	$[1.80, -2.44, 1.69]$	$[2.59, -2.12, 2.00]$	$[2.23, -2.06, 2.15]$
	$[2.10, -9.98, 1.00]$	$[2.89, -9.46, 1.08]$	$[2.53, -9.68, 1.15]$

Table 7: The allowed decay channels for the hidden-bottom $\Sigma_b^{(*)}B^*$ and B_c-like $\Sigma_b^{(*)}\bar{D}^*/\Sigma_c^{(*)}B^*$ molecular pentaquarks.

Systems	(I, J^P)	Waves	Decay channels
$\Sigma_b B^*$	$(1/2, 1/2^-)$	S	$\Lambda_b B$, $\Lambda_b B^*$, $\Sigma_b B$, $\Upsilon(1S)N$, $\Upsilon(1S)N(1440)$, $\Upsilon(2S)N$
		P	$\chi_{b0}(1P)N$, $\chi_{b1}(1P)N$, $h_b(1P)N$, $\chi_{b2}(1P)N$
	$(1/2, 3/2^-)$	S	$\Lambda_b B^*$, $\Upsilon(1S)N$, $\Upsilon(1S)N(1440)$, $\Upsilon(2S)N$
		P	$\chi_{b0}(1P)N$, $\chi_{b1}(1P)N$, $h_b(1P)N$, $\chi_{b2}(1P)N$
		D	$\Lambda_b B$, $\Sigma_b B$
	$(3/2, 1/2^-\|3/2^-)$	S	$\Upsilon(1S)\Delta$
$\Sigma_b^* B^*$	$(1/2, 1/2^-)$	S	$\Lambda_b B$, $\Lambda_b B^*$, $\Sigma_b B$, $\Sigma_b B^*$, $\Upsilon(1S)N$, $\Upsilon(1S)N(1440)$, $\Upsilon(2S)N$
		P	$\chi_{b0}(1P)N$, $\chi_{b1}(1P)N$, $h_b(1P)N$
		D	$\Sigma_b^* B$, $\Upsilon(1D)N$
	$(1/2, 3/2^-)$	S	$\Lambda_b B^*$, $\Sigma_b B^*$, $\Sigma_b^* B$, $\Upsilon(1S)N$, $\Upsilon(1S)N(1440)$, $\Upsilon(2S)N$, $\Upsilon(1D)N$
		P	$\chi_{b0}(1P)N$, $\chi_{b1}(1P)N$, $h_b(1P)N$
		D	$\Lambda_b B$, $\Sigma_b B$
	$(1/2, 5/2^-)$	S	$\Upsilon(1D)N$
		P	$\chi_{b1}(1P)N$, $h_b(1P)N$
		D	$\Lambda_b B$, $\Lambda_b B^*$, $\Sigma_b B$, $\Sigma_b B^*$, $\Sigma_b^* B$, $\Upsilon(1S)N$, $\Upsilon(1S)N(1440)$, $\Upsilon(2S)N$
	$(3/2, 1/2^-\|3/2^-\|5/2^-)$	S	$\Upsilon(1S)\Delta$
$\Sigma_c B^*\|\Sigma_b \bar{D}^*$	$(1/2, 1/2^-)$	S	$\Lambda_c B\|\Lambda_b \bar{D}$, $\Lambda_c B^*\|\Lambda_b \bar{D}^*$, $\Sigma_c B\|\Sigma_b \bar{D}$, $B_c\|\bar{B}_c(0^-)N$, $B_c\|\bar{B}_c(1^-)N$
	$(1/2, 3/2^-)$	S	$\Lambda_c B^*\|\Lambda_b \bar{D}^*$, $B_c\|\bar{B}_c(1^-)N$
		D	$\Lambda_c B\|\Lambda_b \bar{D}$, $B_c\|\bar{B}_c(0^-)N$
	$(3/2, 1/2^-\|3/2^-)$	S	$B_c\|\bar{B}_c(1^-)\Delta$
$\Sigma_c^* B^*\|\Sigma_b^* \bar{D}^*$	$(1/2, 1/2^-)$	S	$\Lambda_c B\|\Lambda_b \bar{D}$, $\Lambda_c B^*\|\Lambda_b \bar{D}^*$, $\Sigma_c B\|\Sigma_b \bar{D}$, $\Sigma_c B^*\|\Sigma_b \bar{D}^*$, $\Sigma_c^* B\|\Sigma_b^* \bar{D}$, $B_c\|\bar{B}_c(0^-)N$, $B_c\|\bar{B}_c(1^-)N$
	$(1/2, 3/2^-)$	S	$\Lambda_c B^*\|\Lambda_b \bar{D}^*$, $\Sigma_c B^*\|\Sigma_b \bar{D}^*$, $\Sigma_c^* B\|\Sigma_b^* \bar{D}$, $B_c\|\bar{B}_c(1^-)N$
		D	$\Lambda_c B\|\Lambda_b \bar{D}$, $\Sigma_c B\|\Sigma_b \bar{D}$, $B_c\|\bar{B}_c(0^-)N$
	$(1/2, 5/2^-)$	D	$\Lambda_c B\|\Lambda_b \bar{D}$, $\Lambda_c B^*\|\Lambda_b \bar{D}^*$, $\Sigma_c B\|\Sigma_b \bar{D}$, $\Sigma_c B^*\|\Sigma_b \bar{D}^*$, $\Sigma_c^* B\|\Sigma_b^* \bar{D}$, $B_c\|\bar{B}_c(0^-)N$, $B_c\|\bar{B}_c(1^-)N$
	$(3/2, 1/2^-)$	S	$B_c\|\bar{B}_c(1^-)\Delta$
	$(3/2, 3/2^-)$	S	$B_c\|\bar{B}_c(0^-)\Delta$, $B_c\|\bar{B}_c(1^-)\Delta$
	$(3/2, 5/2^-)$	D	$B_c\|\bar{B}_c(0^-)\Delta$, $B_c\|\bar{B}_c(1^-)\Delta$

dict two charmed-strange molecular pentaquarks $P_{cs}(3340)$ and $P_{cs}(3400)$, which have the configurations $\Sigma_c\bar{K}^*$ with $(I = 1/2, J^P = 3/2^-)$ and $\Sigma_c^*\bar{K}^*$ with $(I = 1/2, J^P = 5/2^-)$, respectively. These states can be produced through the $\Lambda_b \to P_{cs}^0\bar{D}^0$ decay process in Fig. 1 (b). The production rate is of the same order as that of $P_c(4380)$ and $P_c(4450)$. Hopefully these states can be searched for at LHCb.

In our calculation, we adopt the OPE model, where only one pion exchange is considered. In fact, for these discussed systems, the light vector meson (ρ and ω) exchanges are also allowed. Thus, in future work we can study these systems by one boson exchange (OBE) model by including all allowed light meson exchanges. We also notice the studies by the local hidden gauge approach [4], where the vector light meson exchange is considered, which shows that the vector light meson exchange can provide an attraction. Thus, we can expect that the corresponding Λ value in the OBE model will become smaller than that in OPE model, which means that the light vector meson exchange is helpful to form these discussed molecular states.

Acknowledgments

This project is supported by the National Natural Science Foundation of China under Grants No. 11222547, No. 11175073, No. 11261130311 and 973 program. Xiang Liu is also supported by the National Youth Top-notch Talent Support Program ("Thousands-of-Talents Scheme").

References

[1] H. X. Chen, W. Chen, X. Liu and S. L. Zhu, The hidden-charm pentaquark and tetraquark states, arXiv:1601.02092 [hep-ph].

[2] R. Aaij *et al.* [LHCb Collaboration], Observation of $J\psi$ Resonances Consistent with Pentaquark States in $\Lambda_b^0 \to J/\psi K^- p$ Decays, Phys. Rev. Lett. **115**, 072001 (2015) [arXiv:1507.03414 [hep-ex]].

[3] Z. C. Yang, Z. F. Sun, J. He, X. Liu and S. L. Zhu, The possible hidden-charm molecular baryons composed of anti-charmed meson and charmed baryon, Chin. Phys. C **36**, 6 (2012) [arXiv:1105.2901 [hep-ph]].

[4] J. J. Wu, R. Molina, E. Oset and B. S. Zou, Prediction of narrow N^* and Λ^* resonances with hidden charm above 4 GeV, Phys. Rev. Lett. **105**, 232001 (2010) [arXiv:1007.0573 [nucl-th]].

[5] J. J. Wu, R. Molina, E. Oset and B. S. Zou, Dynamically generated N^* and Λ^* resonances in the hidden charm sector around 4.3 GeV, Phys. Rev. C **84**, 015202 (2011) [arXiv:1011.2399 [nucl-th]].

[6] W. L. Wang, F. Huang, Z. Y. Zhang and B. S. Zou, $\Sigma_c\bar{D}$ and $\Lambda_c\bar{D}$ states in a chiral quark model, Phys. Rev. C **84**, 015203 (2011) [arXiv:1101.0453 [nucl-th]].

[7] C. Garcia-Recio, J. Nieves, O. Romanets, L. L. Salcedo and L. Tolos, Hidden charm N and Delta resonances with heavy-quark symmetry, Phys. Rev. D **87**, 074034 (2013) [arXiv:1302.6938 [hep-ph]].

[8] C. W. Xiao, J. Nieves and E. Oset, Combining heavy quark spin and local hidden gauge symmetries in the dynamical generation of hidden charm baryons, Phys. Rev. D **88**, 056012 (2013) [arXiv:1304.5368 [hep-ph]].

[9] S. G. Yuan, K. W. Wei, J. He, H. S. Xu and B. S. Zou, Study of $qqqc\bar{c}$ five quark system with three kinds of quark-quark hyperfine interaction, Eur. Phys. J. A **48**, 61 (2012) [arXiv:1201.0807 [nucl-th]].

[10] T. Uchino, W. H. Liang and E. Oset, Baryon states with hidden charm in the extended local hidden gauge approach, arXiv:1504.05726 [hep-ph].

[11] R. Chen, X. Liu, X. Q. Li and S. L. Zhu, Identifying exotic hidden-charm pentaquarks, Phys. Rev. Lett. **115**, 132002 (2015) [arXiv:1507.03704 [hep-ph]].

[12] H. X. Chen, W. Chen, X. Liu, T. G. Steele and S. L. Zhu, Towards exotic hidden-charm pentaquarks in QCD, Phys. Rev. Lett. **115**, 172001 (2015) [arXiv:1507.03717 [hep-ph]].

[13] M. Karliner and J. L. Rosner, New Exotic Meson and Baryon Resonances from Doubly-Heavy Hadronic Molecules, Phys. Rev. Lett. **115**, no. 12, 122001 (2015) [arXiv:1506.06386 [hep-ph]].

[14] L. Roca, J. Nieves and E. Oset, LHCb pentaquark as a $\bar{D}^*\Sigma_c - \bar{D}^*\Sigma_c^*$ molecular state, Phys. Rev. D **92**, 094003 (2015) [arXiv:1507.04249 [hep-ph]].

[15] A. Mironov and A. Morozov, Is the pentaquark doublet a hadronic molecule?, JETP Lett. **102**, 271 (2015) [arXiv:1507.04694 [hep-ph]].

[16] J. He, The $\bar{D}\Sigma_c^*$ and $\bar{D}^*\Sigma_c$ interactions and the LHCb hidden-charmed pentaquarks, arXiv:1507.05200 [hep-ph].

[17] U. G. Meissner and J. A. Oller, Testing the $\chi_{c1}\,p$ composite nature of the $P_c(4450)$, Phys. Lett. B **751**, 59 (2015) [arXiv:1507.07478 [hep-ph]].

[18] T. J. Burns, Phenomenology of $P_c(4380)^+$, $P_c(4450)^+$ and related states, arXiv:1509.02460 [hep-ph].

[19] H. Huang, C. Deng, J. Ping and F. Wang, Possible pentaquarks with heavy quarks, arXiv:1510.04648 [hep-ph].

[20] L. Maiani, A. D. Polosa and V. Riquer, The New Pentaquarks in the Diquark Model, Phys. Lett. B **749**, 289 (2015) [arXiv:1507.04980 [hep-ph]].

[21] V. V. Anisovich, M. A. Matveev, J. Nyiri, A. V. Sarantsev and A. N. Semenova, Pentaquarks and resonances in the pJ/ψ spectrum, arXiv:1507.07652 [hep-ph].

[22] G. N. Li, M. He and X. G. He, Some Predictions of Diquark Model for Hidden Charm Pentaquark Discovered at the LHCb, arXiv:1507.08252 [hep-ph].

[23] R. Ghosh, A. Bhattacharya and B. Chakrabarti, The masses of $P_c^*(4380)$ and $P_c^*(4450)$ in the quasi particle diquark model, arXiv:1508.00356 [hep-ph].

[24] Z. G. Wang, Analysis of the $P_c(4380)$ and $P_c(4450)$ as pentaquark states in the diquark model with QCD sum rules, arXiv:1508.01468 [hep-ph].

[25] V. V. Anisovich, M. A. Matveev, J. Nyiri, A. V. Sarantsev and A. N. Semenova, Non-strange and strange pentaquarks with hidden charm, Int. J. Mod. Phys. A **30**, 1550190 (2015) [arXiv:1509.04898 [hep-ph]].

[26] R. F. Lebed, The Pentaquark Candidates in the Dynamical Diquark Picture, Phys. Lett. B **749**, 454 (2015) [arXiv:1507.05867 [hep-ph]].

[27] R. Zhu and C. F. Qiao, Novel Pentaquarks from Diquark-Triquark Model, arXiv:1510.08693 [hep-ph].

[28] F. K. Guo, U. G. Meissner, W. Wang and Z. Yang, Phys. Rev. D **92**, 071502 (2015) [arXiv:1507.04950 [hep-ph]].

[29] X. H. Liu, Q. Wang and Q. Zhao, Understanding the newly observed heavy pentaquark candidates, arXiv:1507.05359 [hep-ph].

[30] M. Mikhasenko, A triangle singularity and the LHCb pentaquarks, arXiv:1507.06552 [hep-ph].

[31] N. N. Scoccola, D. O. Riska and M. Rho, Pentaquark candidates $P_c^+(4380)$ and $P_c^+(4450)$ within the soliton picture of baryons, Phys. Rev. D **92**, 051501 (2015) [arXiv:1508.01172 [hep-ph]].

[32] T. M. Yan, H. Y. Cheng, C. Y. Cheung, G. L. Lin, Y. C. Lin and H. L. Yu, Heavy quark symmetry and chiral dynamics, Phys. Rev. D **46**, 1148 (1992) [Erratum-ibid. D **55**, 5851 (1997)].

[33] M. B. Wise, Chiral perturbation theory for hadrons containing a heavy quark, Phys. Rev. D **45**, 2188 (1992).

[34] G. Burdman and J. F. Donoghue, Union of chiral and heavy quark symmetries, Phys. Lett. B **280**, 287 (1992).

[35] R. Casalbuoni, A. Deandrea, N. Di Bartolomeo, R. Gatto, F. Feruglio and G. Nardulli, Phenomenology of heavy meson chiral Lagrangians, Phys. Rept. **281**, 145 (1997) [arXiv:hep-ph/9605342].

[36] A. F. Falk and M. E. Luke, Strong decays of excited heavy mesons in chiral perturbation theory, Phys. Lett. B **292**, 119 (1992) [arXiv:hep-ph/9206241].

[37] Y. R. Liu and M. Oka, $\Lambda_c N$ bound states revisited, Phys. Rev. D **85**, 014015 (2012) [arXiv:1103.4624 [hep-ph]].

[38] X. Liu, Y. -R. Liu, W. -Z. Deng and S. -L. Zhu, $Z^+(4430)$ as a $D_1' \bar{D}^*$, $(D_1 \bar{D}^*)$ molecular state, Phys. Rev. D **77**, 094015 (2008) [arXiv:0803.1295 [hep-ph]].

[39] D. Y. Chen, X. Liu and T. Matsuki, Two Charged Strangeonium-Like Structures Observable in the $Y(2175) \to \phi(1020)\pi^+\pi^-$ Process, Eur. Phys. J. C **72**, 2008 (2012) [arXiv:1112.3773 [hep-ph]].

[40] Y. s. Oh, T. Song and S. H. Lee, J/ψ absorption by π and ρ mesons in meson exchange model with anomalous parity interactions, Phys. Rev. C **63**, 034901 (2001) [nucl-th/0010064].

[41] A. G. Abrashkevich, D. G. Abrashkevich, M. S. Kaschiev, I. V. Puzynin, FESSDE, a Program for the Finite-element Solution of the Coupled-channel Schrödinger Equation Using High-order Accuracy Approximations, Comput. Phys. Commun. 85, 65 (1995).

[42] A. G. Abrashkevich, D. G. Abrashkevich, M. S. Kaschiev, I. V. Puzynin, FESSDE 2.2: A New Version of a Program for the Finite-element Solution of the Coupled-channel Schrödinger Equation Using High-order Accuracy Approximations, Comput. Phys. Commun. 115, 90 (1998).

[43] H. Yukawa, On the Interaction of Elementary Particles I, Proc. Phys. Math. Soc. Jap. **17**, 48 (1935) [Prog. Theor. Phys. Suppl. **1**, 1].

[44] R. Machleidt, The Meson theory of nuclear forces and nuclear structure, Adv. Nucl. Phys. **19**, 189 (1989).

[45] R. Machleidt, K. Holinde and C. Elster, The Bonn Meson Exchange Model for the Nucleon Nucleon Interaction, Phys. Rept. **149**, 1 (1987).

[46] E. Epelbaum, H. W. Hammer and U. G. Meissner, Modern Theory of Nuclear Forces, Rev. Mod. Phys. **81**, 1773 (2009) [arXiv:0811.1338 [nucl-th]].

[47] B. Aubert *et al.* [BaBar Collaboration], A Study of Excited Charm-Strange Baryons with Evidence for new Baryons $\Xi_c(3055)^+$ and $\Xi_c(3123)^+$, Phys. Rev. D **77**, 012002 (2008) [arXiv:0710.5763 [hep-ex]].

[48] D. Ebert, R. N. Faustov and V. O. Galkin, Masses of excited heavy baryons in the relativistic quark-diquark picture, Phys. Lett. B **659**, 612 (2008) [arXiv:0705.2957 [hep-ph]].

[49] J. J. Wu and B. S. Zou, Prediction of super-heavy N^* and Λ^* resonances with hidden beauty, Phys. Lett. B **709**, 70 (2012) [arXiv:1011.5743 [hep-ph]].